

Metastability Exchange Optical Pumping of Helium-3 at High Pressures and 1.5 T: Comparison of two Optical Pumping Transitions

M. Abboud,* A. Sinatra, G. Tastevin, and P.-J. Nacher

Laboratoire Kastler Brossel, Ecole Normale Supérieure, 24 rue Lhomond, 75005 Paris, France [†]

X. Maître

U2R2M, Université Paris-Sud and CIERM, Hôpital de Bicêtre, 94275 Le Kremlin-Bicêtre Cedex, France [‡]

Abstract:

At low magnetic field, metastability exchange optical pumping of helium-3 is known to provide high nuclear polarizations for pressures around 1 mbar. In a recent paper, we demonstrated that operating at 1.5 T can significantly improve the results of metastability exchange optical pumping at high pressures. Here, we compare the performances of two different optical pumping lines at 1.5 T, and show that either the achieved nuclear polarization or the production rate can be optimized.

PACS numbers: 03.75.Be - 32.60.+i - 32.80.Bx - 67.65.+z - 87.61.-cg

I. INTRODUCTION

Highly polarized helium-3 is used in various fields of science, for example, to perform magnetic resonance imaging (MRI) of air spaces in human lungs [1, 2], or to prepare spin filters for neutrons [3] and polarized targets for nuclear physics [4]. The most successful methods presently used to polarize helium-3 are spin-exchange optical pumping using alkali atoms [5, 6], and pure-helium metastability exchange optical pumping [7, 8]. The applications have driven research towards improvement in terms of photon efficiency, steady-state polarization, and production rate, both for spin exchange optical pumping [9], and metastability exchange optical pumping [3, 10]. The metastability exchange technique was demonstrated by Colegrove, Scheerer, and Walters over forty years ago [7]. In standard conditions, metastability exchange optical pumping is performed at low pressure (1 mbar) in a guiding magnetic field up to a few mT. Metastable 2^3S -state atoms are produced using a radiofrequency discharge. They are optically pumped using the 2^3S - 2^3P transition at 1083 nm. The electronic polarization is transferred to the nuclei by hyperfine interaction. Through metastability exchange collisions, nuclear polarization is transferred to ground state helium-3 atoms. Metastability exchange optical pumping in standard conditions provides in a few seconds high nuclear polarizations (up to 90% at 0.7 mbar [11]). Unfortunately, the achieved nuclear polarization rapidly drops down when the helium-3 pressure exceeds a few mbar [10, 12]. Therefore, a delicate polarization-preserving compression stage

is necessary for all applications needing a dense sample.

We recently demonstrated that operating at 1.5 T can significantly improve the nuclear polarization achieved at high pressures [13], using one of the most intense lines in the 2^3S - 2^3P absorption spectrum. Here, we show that a different choice of optical pumping transition can further improve the steady-state polarization although the production rate is slightly lower. We also describe more precisely the experimental protocol, and demonstrate the consistency of the optical absorption technique for dynamic measurement of the nuclear polarization in presence of the optical pumping laser.

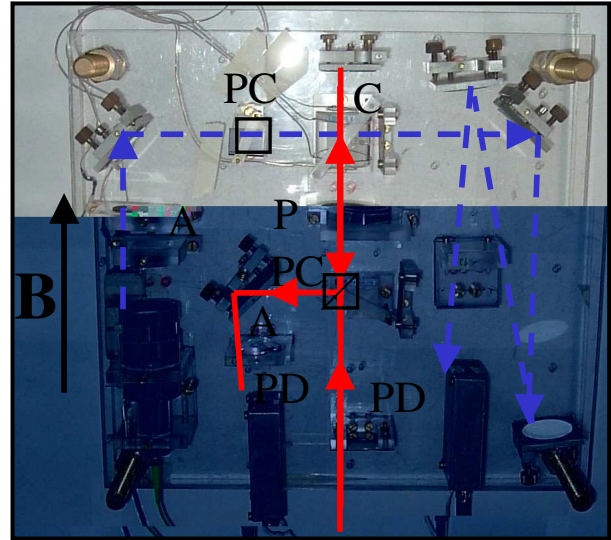


FIG. 1: Picture of the experimental apparatus of optical pumping at 1.5 T, containing the optical elements and the sealed optical pumping cell. The pump laser beam (solid arrow) is parallel to the magnetic field \mathbf{B} , and the probe laser beam (dashed arrow) is perpendicular to the magnetic field. C: optical pumping cell, PC: polarizing cube, P: quarter-wave plate, PD: photodiode, A: attenuator.

[†]Laboratoire Kastler Brossel is a unité de recherche de l'Ecole Normale Supérieure et de l'Université Pierre et Marie Curie, associée au CNRS (UMR 8552).

[‡]U2R2M (Unité de Recherche en Résonance Magnétique Médicale) is a unité de recherche de l'Université Paris-Sud, associée au CNRS (UMR 8081).

*Electronic address: marie.abboud@lkb.ens.fr

II. EXPERIMENTAL

A. Setup

Experiments are performed in the bore of a clinical MRI scanner providing a homogeneous 1.5 T magnetic field. The experimental apparatus is shown in Fig.1. The helium-3 gas is enclosed in a sealed cylindrical Pyrex cell, 5 cm in diameter and 5 cm in length. Cells filled with pressure $P=1.33, 8, 32,$ and 67 mbar of pure helium-3 are used. A radiofrequency high voltage applied to electrodes on the outside of the cell generates a weak electrical discharge in the gas. It is used to populate the 2^3S state and maintain a metastable atoms density n_m in the range $1-8 \times 10^{10}$ atoms/cm³, depending on the applied voltage and the gas pressure. The optical pumping laser is a 50 mW single mode laser diode amplified by a 0.5 W ytterbium-doped fiber amplifier [14]. The laser wavelength can be tuned by temperature control over the entire spectrum of the 2^3S-2^3P transition of helium (~ 150 GHz at 1.5 T, see Fig.2). The circular polarization of the pump beam is obtained using a combination of polarizing cube and quarter-wave retarding plate. The pump beam is back-reflected after a first pass in the cell to enhance its absorption, and collected by a photodiode to measure its absorption. The probe beam is provided by another single mode laser diode. It is attenuated and linearly polarized perpendicularly to the magnetic field. The absorption of probe and pump lasers are measured using a modulation technique. The discharge intensity is modulated at 133 Hz and the absorptions are measured with lock-in amplifiers. The average values of the transmitted probe and pump intensities are also recorded. Laser sources and electronics remain several meters away from the magnet bore in a low-field region.

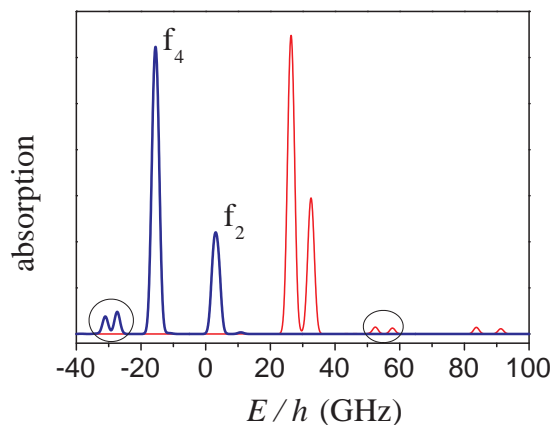


FIG. 2: Computed absorption spectra for σ^- (thick line) and σ^+ (thin line) light at 1.5 T. f_4 and f_2 are the two optical pumping lines used in our experiments. The circled peaks on the left (respectively on the right) correspond to the probe lines used when the pump laser is tuned on f_4 (respectively on f_2). Spectral line positions are defined as in reference [15].

B. Optical pumping configuration

The structure of the 2^3S-2^3P transition and Zeeman sublevels of helium-3 at 1.5 T is described in [13, 15]. In our experiments, optical pumping is performed using one of the two σ^- pumping lines labeled f_4 or f_2 in the absorption spectrum displayed in Fig.2. The f_4 line consists of four unresolved transitions spreading over 1.31 GHz. Given the Doppler width of helium-3 at room temperature (2 GHz FWHM), it addresses simultaneously four metastable sublevels A_1 to A_4 with $m_F=-3/2, -1/2$ and $1/2$, where m_F is the magnetic quantum number for the total angular momentum (see Fig.3). The f_2 line (two transitions split by 1.37 GHz) simultaneously addresses sublevels A_5 and A_6 with $m_F=1/2$ and $3/2$. The population transfer into A_5 and A_6 for f_4 pumping (or into A_1 to A_4 for f_2 pumping) occurs as follows: excitation

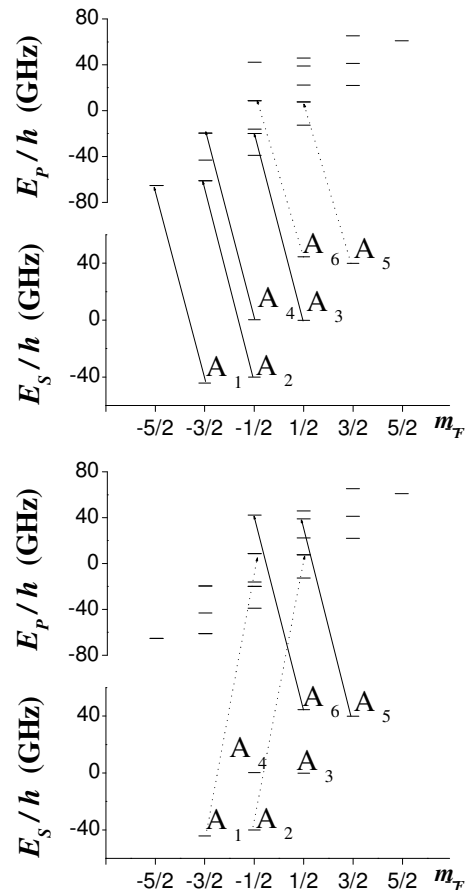


FIG. 3: Energies and magnetic quantum numbers m_F of the helium-3 sublevels at 1.5 T for the 2^3S (E_S) and 2^3P (E_P) states. The upper (lower) scheme corresponds to the f_4 (f_2) optical pumping configuration. The σ^- pumping transitions (solid lines) are displayed. The populations of the sublevels A_5 and A_6 (A_1 and A_2) not addressed by the f_4 (f_2) optical pumping transition are measured using the σ^- (σ^+) probe transitions (dashed lines). Level names A_1 to A_6 and energy zeroes are defined as in reference [15].

by laser absorption, collisional redistribution in the 2^3P state, and spontaneous emission.

C. Optical measurement of nuclear polarization

The optical detection method used in our experiments is based on absorption measurements using a weak probe beam. This absorption technique does not need any calibration and can be used at arbitrary magnetic field, and pressure [15]. It relies on the fact that in the absence of optical pumping, metastability exchange collisions impose a spin temperature distribution for the metastable populations $a_{mF} \propto e^{\beta m_F}$, where $1/\beta$ is the spin temperature in the 2^3S state related to the nuclear polarization M in the ground state $M = (e^\beta - 1)/(e^\beta + 1)$.

In practice, the probe laser frequency is swept over two lines. Peaks amplitudes are precisely measured by a fit to a Voigt absorption profile. The population ratio of the two hyperfine sublevels addressed by the probe lines is then found using the field-dependent computed transition probabilities, and is used to calculate the spin temperature. Hence, the ground-state nuclear polarization M is inferred [15].

Polarization build-up is monitored in the presence of

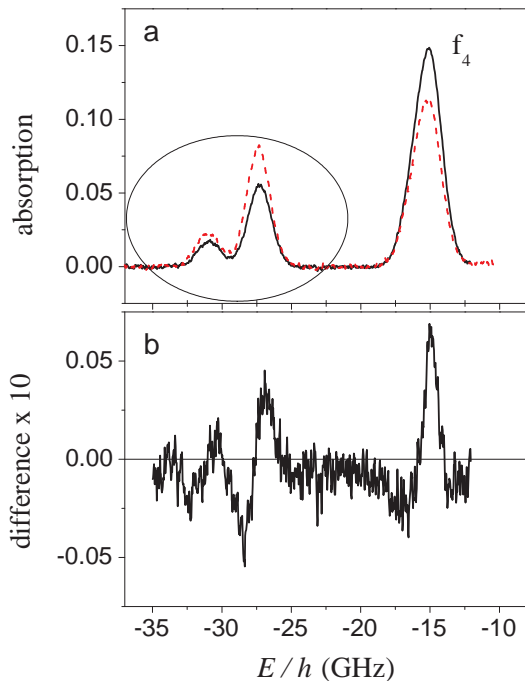


FIG. 4: **a:** Absorption signals recorded with pump laser on (dashed line) and off (solid line). They are performed in the 8 mbar cell with 0.25 W pump laser power for f_4 pumping after reaching $M_{eq} = 0.43$. The circled peaks involving sublevels A_5 and A_6 , not addressed by the pump laser, are used to compute M . **b:** The lower graph is a residue plot showing the difference between the solid line data in Fig.4a and a computed spin temperature distribution spectrum.

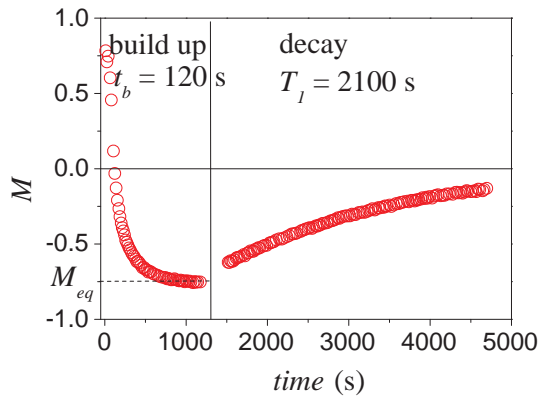


FIG. 5: Example of dynamic monitoring of the nuclear polarization M in the 8 mbar cell. Starting from a gas prepared with $M > 0$ at time $t = 0$, the pump laser is tuned on the f_2 line with 0.5 W power. After reaching the steady-state nuclear polarization $M_{eq} = -0.75$, the pump laser is turned off at $t = 1300$ s, and the discharge-induced decay of the polarization is observed.

the optical pumping beam. Therefore, the probe absorption measurements must involve metastable sublevels not addressed by the optical pumping laser. In our configuration (see Fig.3), the populations of sublevels A_5 and A_6 (respectively A_1 and A_2) are measured for f_4 (respectively f_2) pumping. Fig.4a shows typical absorption spectra recorded in the absence and in the presence of the pump laser. In the absence of the pump laser (solid line), the spectrum is accurately fit by the spectrum computed assuming a spin temperature distribution (residue plot in Fig.4b). The presence of the pump strongly affects the population distribution, with efficient population transfer from the pumped levels to A_5 and A_6 and modifies the absorption profile (dashed line). However the ratio of populations in sublevels A_5 and A_6 remains unaffected, and an absorption measurement still accurately provides the correct value for M .

An example of dynamical measurement of polarization build-up and decay is shown in Fig.5 for the 8 mbar cell. Several scans of the probe laser are recorded successively, and the value of the nuclear polarization M is inferred as a function of time. The gas is initially polarized to the equilibrium positive value of M achieved with f_4 pumping. At time $t = 0$, the pump laser is tuned to the f_2 line. When the new steady-state polarization M_{eq} is reached, the pump laser is turned off and polarization decays by discharge-induced relaxation.

III. RESULTS

Several experimental parameters influence the performances of optical pumping: the cell geometry, the gas pressure, the discharge conditions (voltage, electrodes configuration) which impact on T_1 and n_m , the optical pumping transition, and the pump laser power. A sys-

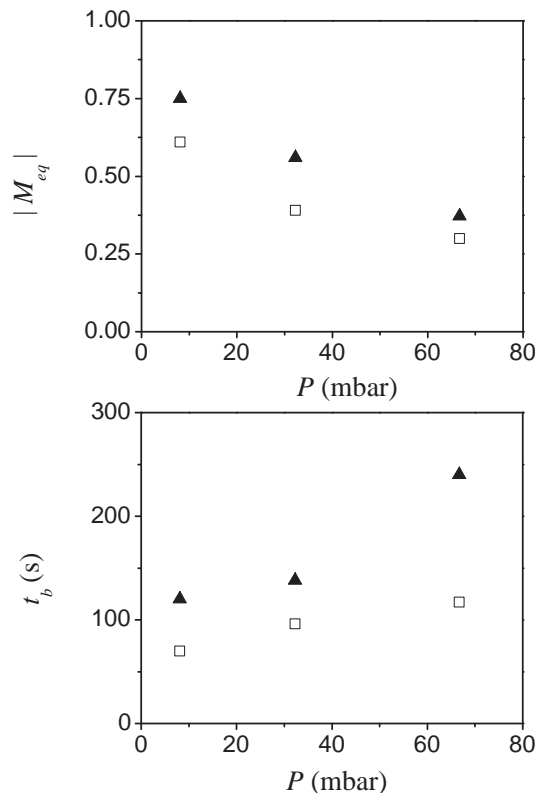


FIG. 6: Absolute values of steady-state nuclear polarizations M_{eq} and polarization build-up times t_b as a function of the helium-3 pressure at 1.5 T. Triangles (respectively squares) are data obtained when the pump laser (0.5 W) is tuned to f_2 (respectively f_4). The measured n_m and T_1 are: at 8 mbar, 3.54×10^{10} at./cm³ and 2100 s, at 32 mbar, 2.47×10^{10} at./cm³ and 1490 s, at 67 mbar, 1.30×10^{10} at./cm³ and 1190 s.

tematic study of optical pumping using the f_4 line has been reported in [13]. Here, we focus on the comparison of optical pumping with f_4 and f_2 lines in the same cells. We present selected results obtained with identical discharge conditions for f_4 and f_2 , using a 0.5 W pump power.

The f_2 line yields higher steady-state polarizations but f_4 allows pumping with significantly shorter build-up times (Fig.6). As a result, the magnetization production rates $R_a = P \times M_{eq}/t_b$ are slightly lower for f_2 (see Table I). The main difference between the two optical

pumping lines actually lies in the photon efficiency, defined as the number of polarized nuclei per photon absorbed by the gas. A simple calculation, based on the average angular momentum transfer from polarized light to atoms during one absorption-collisional redistribution-spontaneous emission cycle, shows that the photon efficiency of f_2 should be approximately twice that of f_4 . This has been experimentally checked, at various laser powers. Magnetization production rates for f_2 pumping are yet slightly lower due to the lower absorption of the pump beam on this line with respect to f_4 .

TABLE I: Magnetization production rates $R_a = P \times M_{eq}/t_b$ versus gas pressure (data in Fig.6).

P (mbar)	R_a (mbar/s)	
	f_4	f_2
8	0.07	0.05
32	0.13	0.12
67	0.17	0.11

IV. DISCUSSION

We have compared the performances of two different optical pumping lines at 1.5 T in helium-3 gas, at high pressures (up to 67 mbar). The strongest line of the σ^- absorption spectrum (f_4) yields the highest magnetization production rates. However, the highest steady-state nuclear polarizations (up to $M_{eq} = -0.75$ at 8 mbar) are achieved using a weaker line with higher photon efficiency. f_2 pumping, requiring fewer absorbed photons to achieve the same production rate, is thus advantageous when long, optically thick pumping cells are used.

Given the structure of sublevels and optical transitions, one could expect that the two most intense σ^+ lines would be just as efficient as the corresponding σ^- lines. Similar optical pumping performances have indeed been obtained, although no systematic comparison has been carried out.

An analysis of all optical pumping data collected at 1.5 T is under way using a detailed model of metastability exchange optical pumping in high field conditions, and will be the subject of a forthcoming paper.

-
- [1] M.S. Albert et al., 1994, Nature **370**, 199.
 - [2] H. Möller et al., 2002, Magn. Res. in Medicine **47**, 1029.
 - [3] J. Becker et al., 1998, Nucl. Instrum. Meth. A **402**, 327.
 - [4] W. Xu et al., 2000, Phys. Rev. Lett. **85**, 2900.
 - [5] M.A. Bouchiat et al., 1960, Phys. Rev. Lett. **5**, 373.
 - [6] T.G. Walker, W. Happer, 1997, Rev. Mod. Phys. **69**, 629.
 - [7] F. D. Colegrove et al., 1963, Phys. Rev. **132**, 2561.
 - [8] P.-J. Nacher et al., 1985, J. Physique **46**, 2057.
 - [9] E. Babcock et al., 2003, Phys. Rev. Lett. **91**, 123003.
 - [10] T.R. Gentile, R.D. Mckeown, 1993, Phys. Rev. A **47**, 456.
 - [11] M. Batz et al., 2004, NIST Journal of Research, Proceed. Precis. Meas. with Slow Neutrons, in press.
 - [12] P.-J. Nacher et al., 2000, Acta Phys. Pol. B **33**, 2225.
 - [13] M. Abboud et al., 2004, to appear in Europhys. Lett..
 - [14] S.V. Chernikov et al., 1997, Electr. Lett. **33**, 787.
 - [15] E. Courtade et al., 2002, Eur. Phys. J. D **21**, 25.